ACS APPLIED MATERIALS & INTERFACES

Research Article

www.acsami.org

Fluorescent pH Sensor Based on Ag@SiO_2 Core–Shell Nanoparticle

Zhenhua Bai,[†] Rui Chen,[‡] Peng Si,[†] Youju Huang,[†] Handong Sun,[‡] and Dong-Hwan Kim*,[†]

[†]School of Chemical and Biomedical Engineering, Nanyang Technological University, 637457, Singapore

[‡]School of Physical and Mathematical Sciences, Nanyang Technological University, 637371, Singapore

Supporting Information

ABSTRACT: We have demonstrated a novel method for the preparation of a fluorescence-based pH sensor by combining the plasmon resonance band of Ag core and pH sensitive dye (HPTS). A thickness-variable silica shell is placed between Ag core and HPTS dye to achieve the maximum fluorescence enhancement. At the shell thickness of 8 nm, the fluorescence intensity increases 4 and 9 times when the sensor is excited at 405 and 455 nm, respectively. At the same time, the fluorescence intensity shows a good sensitivity toward pH value in the range of 5–9, and the ratio of emission intensity at 513 nm excited at 455 nm to that excited at 405 nm versus the pH value in the range of 5–9 is determined. It is believed that the present pH sensor has the potential for determining pH real time in the biological sample.

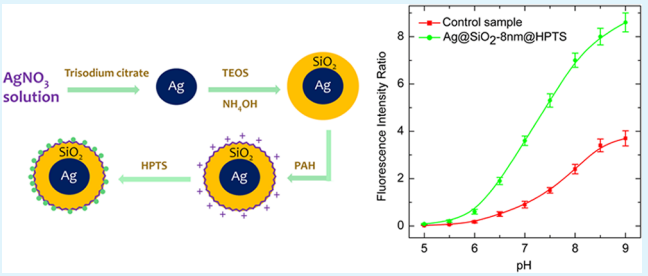

KEYWORDS: *pH sensor, fluorescence enhancement, HPTS, Ag nanoparticle, plasmon resonance, core–shell*

1. INTRODUCTION

Intracellular pH value is an essential parameter for cell, enzyme, and tissue activities,[1] as abnormal intracellular pH values associated with inappropriate cell function and growth may give rise to various diseases, such as cancers and neurological disorders.[2] Therefore, the accurate determination of intracellular pH is of great interest in molecular science, biomedicine, and bioprocess applications.[3] Among several techniques developed to measure a pH value in live cells,[4] fluorescence spectroscopy has drawn much attention because their high temporal/spatial resolution, minimal invasiveness, and applicability to a wide variety of cells.[5] To this end, a fluorescent pH-sensitive dye, 8-hydroxypyrene-1,3,6-trisulfonic acid (HPTS), also named as pyranine, has been demonstrated as a suitable intracellular pH sensor due to a number of advantageous features over other optical materials, such as low toxicity, minimal interference with cell, high resolution, and rapid response.[6−8] Despite such attractive features, the fluorescence efficiency of the HPTS is strongly dependent on the pH value of solutions, which decreases to less than 1% in acidic conditions, hampering their practical applications, particularly when used for deep tissue and low concentration detection.[9] Therefore, it is highly needed to enhance the fluorescence intensity of the HPTS to improve the sensitivity and accuracy of the pH sensor. However, up until now, there has been no study on the fluorescence enhancement of HPTS dye.

Noble metals have been demonstrated to enhance fluorescence of rare-earth ions, organic dyes, and quantum dots using the resonant coupling between the surface plasmon resonance bands of metals and absorption or emission band of fluorescent materials, which is known as metal enhanced fluorescence.[10−12] Among the noble metals, silver has been recognized as an attractive fluorescence enhancer, because of its narrow plasmon band and high scattering efficiency.[13,14] Core–shell structures have been reported as an effective mean to improve the stability of silver nanostructures,[15,16] as well as to provide a spacer to control the distance between metal enhancer and fluorophore for optimized fluorescence efficiency.[17,18]

Inspired by metal enhanced fluorescence, we have, in this work, investigated the fluorescence property and pH sensitivity of HPTS dye with the assistance of Ag nanoparticles. We fabricated a fluorescent pH sensor based on the metal-spacer-fluorophore approach, and systematically increased the spacer thickness to study the fluorescence property of the HPTS-adsorbed Ag@SiO_2 nanoparticles (Ag@SiO_2@HPTS). Because of the enhanced fluorescence achieved by optimized spacer thickness and proper excitation wavelength, the pH sensitivity and accuracy of present pH sensor can be highly improved.

2. EXPERIMENTAL SECTION

2.1. Chemicals. All the chemicals were purchased from Sigma-Aldrich and used without further purification; Silver nitrate ($AgNO_3$), trisodium citrate dihydrate ($Na_3C_6H_5O_7.2H_2O$), tetraethylorthosilicate (TEOS), ammonium hydroxide, absolute ethanol, sodium hydroxide (NaOH), hydrochloric acid (HCl), poly(allyamine hydrochloride) (PAH), and 1-hydroxypyrene-3,6,8-trisulfonic acid (HPTS). Nanopure water (>18.0 MΩ) purified using the Milipore Milli-Q gradient system, was used in all experiments. All the glass apparatus were cleaned in aqua regia solution before being used.

Received: April 25, 2013
Accepted: May 28, 2013
Published: May 28, 2013

2.2. Preparation of HPTS-Adsorbed Ag@SiO_2. As illustrated in Figure 1, the HPTS-adsorbed Ag@SiO_2 was fabricated in four steps.

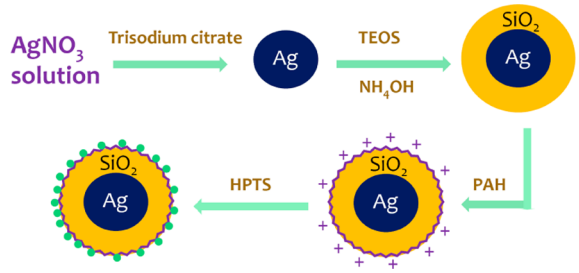

Figure 1. Schematic representation of the preparation of HPTS-adsorbed Ag@SiO_2 Nanoparticles.

(1) Ag nanoparticles were prepared by the reduction of silver nitrate by trisodium citrate. (2) Ag@SiO_2 nanoparticles were obtained by the hydrolysis and condensation of TEOS on the surface of Ag nanoparticles. (3) The negatively charged silica surface was modified by positively charged PAH. (4) HPTS with sulfonic acid groups was immobilized via electrostatic interaction on cationic supports of Ag@SiO_2 nanoparticles.

2.2.1. Synthesis of Ag Nanoparticles. Silver nanoparticles were prepared by a modified version of the procedure described previously.[19] 18 mg of $AgNO_3$ was dissolved in 98 mL of water, and then heated to 140 °C within 30 min under vigorous stirring. Two milliliters of freshly prepared 34 mM trisodium citrate was added into the $AgNO_3$ solution within 2 min, and the mixture was kept under stirring at 140 °C. After being stirred for 1 h, the reaction solution was cooled to room temperature.

2.2.2. Fabrication of Ag@SiO_2 Core–Shell Nanoparticles. The SiO_2 coating on Ag nanoparticles was realized by a Stober method.[20] The prepared Ag nanoparticles (3 mL) were added to a mixture of absolute ethanol (100 mL, 99.9%), ammonium hydroxide (1.5 mL, 28 wt %), and pure H_2O (3.75 mL). After 20 min of ultrasonication, various amounts of TEOS (2–50 μL) were added dropwise, and the mixture was stirred for 12 h at room temperature. The thickness of silica coatings could be controlled by adjusting the amount of the TEOS. The suspension was separated by centrifugation and washed by ethanol three times. The obtained Ag@SiO_2 nanoparticles were redispersed in deionized water before further use.

2.2.3. HPTS Adsorption on Ag@SiO_2. Three hundred microliters of PAH was added to the aqueous solution of Ag@SiO_2 nanoparticles, and the resultant solution was stirred for 6 h. During this incubation period, the positively charged PAH was adsorbed to the silica surface by electrostatic interaction. The excess PAH was separated by ultracentrifugation at a speed of 8000 rpm. The PAH-coated Ag@SiO_2 was washed with deionized water twice and redispersed in 10 mL of deionized water. Finally, 100 μL of HPTS solution (2 mM) was added to the aforementioned solution, and stirred for 4 h, resulting in negatively charged HPTS adsorbed on the surface of PAH-coated Ag@SiO_2.

2.3. Characterization. A pH meter (BOECO, BT-600, Germany) was used for the measurement of pH values. Solutions in the pH range of 5–9 were prepared by diluting 0.1 mol/L of hydrogen chloride or 0.1 mol/L of sodium hydroxide. The structural properties of prepared products were characterized by a field emission scanning electron microscopy (FE-SEM) (JSM-6700F at an acceleration voltage of 5 kV) and a transmission electron microscope (TEM) (JEOL TEM 2010 microscope operating at 200 kV). Ultraviolet–visible (UV–vis) absorption spectra were recorded by Shimadzu UV-2450 spectrophotometer. Fluorescence measurements were carried out using a Shimadzu RF-5301PC spectrophotometer. All measurements were performed at room temperature.

3. RESULTS AND DISCUSSION

3.1. Structural Properties of Ag@SiO_2 Core–Shell Nanoparticle. Trisodium citrate-reduced silver nanoparticles (57 ± 5 nm) were prepared for maximum fluorescence enhancement (Figure 2a).[21] To obtain the highest emission

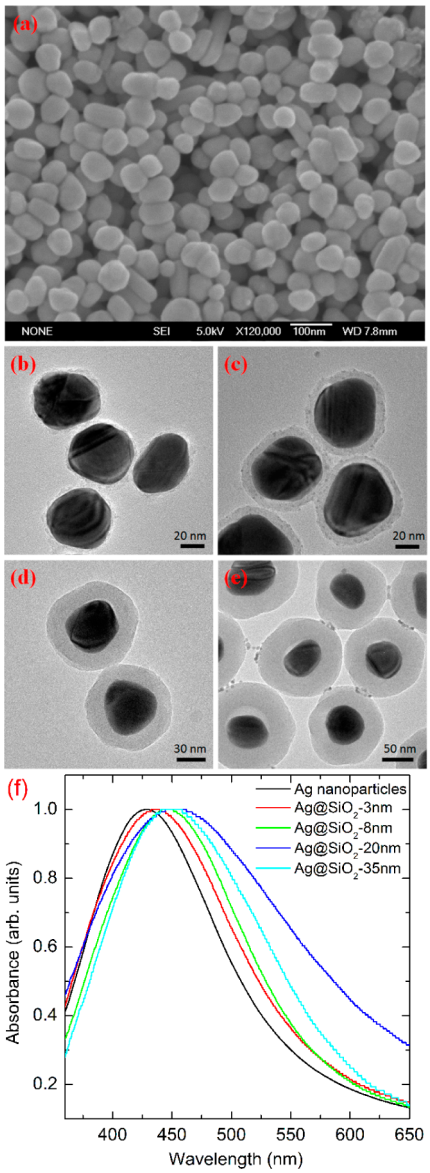

Figure 2. (a) FE-SEM image of Ag nanoparticles. TEM images of Ag@SiO_2 nanoparticles with the shell thickness of (b) 3 ± 1, (c) 8 ± 1, (d) 20 ± 2, and (e) 35 ± 3 nm. (f) UV–visible spectra of Ag nanoparticles and Ag@SiO_2 nanoparticles with different silica spacer thicknesses.

enhancement, various thicknesses of silica shell are prepared using different amounts of TEOS (2–50 μL). As a result, Ag@SiO_2 nanoparticles with various shell thicknesses of 3 ± 1 nm (Figure 2b), 8 ± 1 nm (Figure 2c), 20 ± 2 nm (Figure 2d), and 35 ± 3 nm were obtained (Figure 2e). The size distribution of the synthesized nanoparticles is shown in Figure S1 in the Supporting Information. The silica shell can not only adjust the distance between Ag core and the exterior emitter but also improve the colloidal and chemical stability of the metal enhancer.[15]

Figure 2f presents the absorbance spectra of bare Ag nanoparticles and Ag@SiO_2 core−shell nanoparticles with different silica thicknesses. The increase in silica shell thickness causes the redshift of the plasmon resonance band from 428 to 458 nm because of large refractive index of the silica shell and the decreased plasmon oscillation energy,[22] which is in good agreement with a previous report.[23,24]

3.2. Optical Properties of HPTS-Adsorbed Ag@SiO_2 Core−Shell Nanoparticles. The HPTS molecule has two absorption bands at 405 and 455 nm, and the absorption maximum exhibits a shift from 405 nm in acidic conditions to 455 nm in basic conditions (see the Supporting Information, Figure S2). Figure 3a shows the fluorescence emission spectra of HPTS-adsorbed Ag@SiO_2 with varied silica thicknesses. A control sample was prepared by the immobilization of the HPTS on the surface of silica nanoparticle (diameter of 60 nm) to evaluate the effect of Ag core. The amount of the adsorbed dyes on the nanoparticles with various silica thicknesses likely increases with the increase in the size of nanoparticles. Therefore, the absorbance of supernatants was monitored to estimate the unbound dye left in the supernatants; the number of HPTS on Ag@SiO_2-3 nm, Ag@SiO_2-8 nm, Ag@SiO_2-20 nm, and Ag@SiO_2-35 nm were estimated to be about 100, 110, 150, and 180, respectively. When excited at 405 nm, all samples show broad green emissions in the range of 470−620 nm with the peak wavelength of 513 nm, which is the characteristic emission of HPTS (see the Supporting Information, Figure S3). At the silica shell thickness of 3 nm, the emission intensity of HPTS is even lower than that of the control sample, probably due to the increased nonradiative decay caused by Ag core.[25] The maximum emission enhancement was achieved at the shell thickness of 8 nm. Further increase in shell thickness results in the decrease of the emission intensity because the surface plasmon of Ag core does not effectively interact with HPTS due to the thick silica barrier. Similarly, both quenching and enhancement of fluorescent emission are also observed when excited at 455 nm (Figure 3b), indicating precise tuning of distance between metal core and fluorophore is vital to achieve the highest fluorescence enhancement. In this work, the maximum fluorescence enhancement is achieved at the shell thickness of 8 nm for both excitation wavelengths. Two processes are generally responsible for the fluorescence enhancement by metal nanostructures.[26] One process occurs during the absorption stage and the other takes place during the emission stage. When a fluorophore is located near metal nanostructures and the excitation light is resonant with the plasmon mode of metal nanostructures, enhanced local electric fields are generated at the position of the fluorophore, resulting in an enhancement of absorption efficiency. On the other hand, the enhanced local electric fields at the fluorescence frequency result in an enhancement of radiative decay rate when the emitted light is resonant with the plasmon mode of metal nanostructures. As a result, the total optical enhancement of the emitter is determined by both the absorption enhancement and the emission enhancement. As the plasmon resonance bands of a series of Ag@SiO_2 nanocomposites cover both excitation wavelength and emission band of the HPTS dye, the fluorescence enhancement in our samples likely comes from both absorption and emission enhancement.

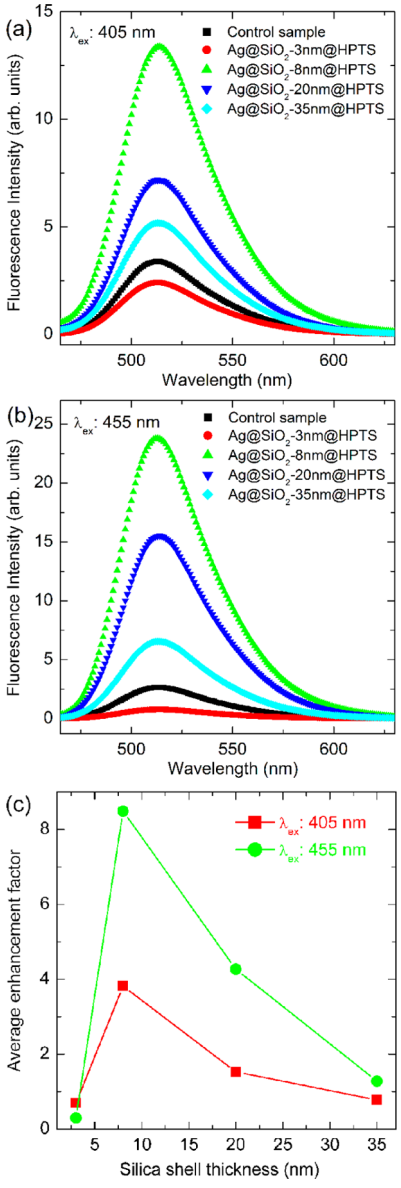

Figure 3. Fluorescence spectra of HPTS adsorbed Ag@SiO_2 nanoparticles with various shell thicknesses, when excited by (a) 405 and (b) 455 nm, respectively. Fluorescence spectra of control sample are also shown for the purpose of comparison. (c) Average fluorescence enhancement factor of HPTS adsorbed Ag@SiO_2 nanoparticles relative to silica nanospheres as the function of silica spacer thickness.

To study the fluorescence enhancement of a single HPTS on different shell thicknesses and excitation wavelengths, we calculated the average enhancement factors by dividing the fluorescence intensity by the number of the adsorbed dyes. The maximum enhancement at the excitation of 455 nm is more than two times stronger than that at 405 nm. The variation in fluorescence enhancement factor at different excitation wavelengths can be explained by examining the plasmon resonance bands of these nanoparticle samples; the plasmon resonance band of HPTS-adsorbed Ag@SiO_2 nanoparticles at 455 nm is much stronger than that at 405 nm (Figure 2f).

3.3. pH Sensitivity of HPTS-Adsorbed Ag@SiO_2 Core−Shell Nanoparticle. To investigate the pH sensitivity of our samples, the fluorescence spectra of HPTS-adsorbed Ag@SiO_2-8 nm are measured in the pH range of 5−9. As shown in panels a and b in Figure 4, with the increase of pH value from 5 to 9, the emission intensity gradually decreases by half upon the excitation of 405 nm. In contrast, 50-fold fluorescence

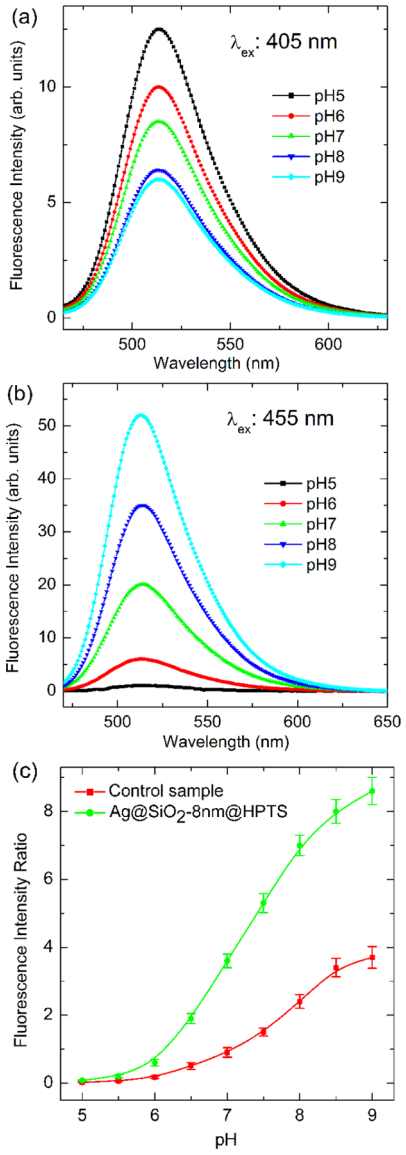

Figure 4. Fluorescence spectra of HPTS-adsorbed Ag@SiO_2-8 nm nanoparticles in pH range of 5−9, when excited by (a) 405 and (b) 455 nm, respectively. (c) Intensity ratio of HPTS-adsorbed Ag@SiO_2-8 nm sample detected at 513 nm (λ_{ex} = 455 nm/λ_{ex} = 405 nm) in pH range of 5−9.

enhancement is observed when the excitation is changed to 455 nm. The above results strongly indicate that the fluorescence intensity of the prepared nanoparticles is very sensitive to the variation of pH value in solution.

Because fluorescence signals can be influenced by tissue geometry, excitation power, dye concentration, photobleaching, and optical characteristics of tissue,[27] a ratiometric calibration using a double excitation[7] has been introduced to obviate these problems. The ratio calculated by dividing a fluorescence obtained from one excitation wavelength by that obtained from another excitation can generally eliminate the effects of variable probe concentration quenching, path length and photo bleaching on signal strength. For the HPTS, each excitation wavelength produces fluorescence emission centered at 513 nm, and the emission intensity is strongly pH dependent (see the Supporting Information, Figure S4). Therefore, using a predetermined calibration curve, ratio data can be transformed to pH data. Figure 4c depicts the intensity ratio of the HPTS-adsorbed Ag@SiO_2-8 nm sample detected at 513 nm (λ_{ex} = 455 nm/λ_{ex} = 405 nm) in pH range of 5−9. The intensity ratios of the control sample are also shown for the purpose of comparison. Although a slight change of the intensity ratio is observed in the pH ranges of 5−6 and 8−9, a steep and linear change can be seen in the pH range of 6−8, overall exhibiting excellent linear response of the fluorescence intensity ratio. We note that although the release of adsorbed HPTS from the shell surface was detected when the pH value is above 9.5, the present pH sensor showed high stability in the pH range of 5−9. In addition, the pH sensitivity of the HPTS-adsorbed Ag@SiO_2 was significantly enhanced compared with the control. The fluorescent intensity ratio plot of HPTS-adsorbed Ag@SiO_2 relative to the control implies that pH sensitive region is unchanged by the adoption of core−shell structure.

4. CONCLUSIONS

A novel pH sensor consisting of a Ag core, a silica spacer, and HPTS dyes is developed in metal-spacer-fluorophore format. The fluorescence intensity of HPTS dyes was strongly dependent on the silica spacer thickness and excitation wavelength. At the shell thickness of 8 nm, maximum fluorescence enhancements of 4 and 9 times were achieved when excited by 405 and 455 nm, respectively. The ratio of emission intensity at 513 nm excited at 455 nm to that excited at 405 nm is correlated well with the pH value of aqueous solution, over the pH range of 5−9. The pH sensitivity and linearity are demonstrated over the physiological region. The excellent structural and optical properties make these core−shell nanoparticles promising in application as intracellular pH sensor.

■ ASSOCIATED CONTENT

Supporting Information

Size distributions of Ag core, and Ag@SiO_2 nanoparticles; absorption spectra of HPTS solution in the pH range of 2−12; fluorescence spectra of HPTS dye at the excitation of 405 and 455 nm; structure and graphical representation of HPTS dye in acid and basic condition. This material is available free of charge via the Internet at http://pubs.acs.org.

■ AUTHOR INFORMATION

Corresponding Author

*E-mail: dhkim@ntu.edu.sg.

Notes

The authors declare no competing financial interest.

■ ACKNOWLEDGMENTS

This work was supported by a research grant from National Medical Research Council from Singapore (NMRC/EDG/1060/2012).

■ REFERENCES

(1) Weinlich, M.; Heydasch, U.; Mooren, F.; Starlinger, M. *Res. Exp. Med.* **1998**, *198*, 73−82.
(2) Han, J. Y.; Burgess, K. *Chem. Rev.* **2010**, *110*, 2709−2728.
(3) Kermis, H. R.; Kostov, Y.; Harms, P.; Rao, G. *Biotechnol. Prog.* **2002**, *18*, 1047−1053.
(4) Kermis, H. R.; Kostov, Y.; Rao, G. *Analyst* **2003**, *128*, 1181−1186.
(5) Clement, N. R.; Gould, J. M. *Biochemistry* **1981**, *20*, 1534−1538.

(6) Amali, A. J.; Singh, S.; Rangaraj, N.; Patra, D.; Rana, R. K. *Chem. Commun.* **2012**, *48*, 856−858.
(7) Kano, K.; Fendler, J. H. *Biochim. Biophys. Acta* **1978**, *509*, 289−299.
(8) Overly, C. C.; Lee, K. D.; Berthiaume, E.; Hollenbeck, P. J. *Proc. Natl. Acad. Sci. U.S.A.* **1995**, *92*, 3156−3160.
(9) Gutman, M.; Nachliel, E.; Moshiach, S. *Biochemistry* **1989**, *28*, 2936−2940.
(10) Jin, Y. D.; Gao, X. H. *Nat. Nanotechnol.* **2009**, *4*, 571−576.
(11) Tam, F.; Goodrich, G. P.; Johnson, B. R.; Halas, N. J. *Nano Lett.* **2007**, *7*, 496−501.
(12) Zhang, H.; Li, Y. J.; Ivanov, I. A.; Qu, Y. Q.; Huang, Y.; Duan, X. F. *Angew. Chem., Int. Ed.* **2010**, *49*, 2865−2868.
(13) Kerker, M.; Blatchford, C. G. *Phys. Rev. B* **1982**, *26*, 4052−4064.
(14) Mulvaney, P. *Langmuir* **1996**, *12*, 788−800.
(15) Li, C. Y.; Zhu, Y. H.; Zhang, X. Q.; Yang, X. L.; Li, C. Z. *Rsc. Adv.* **2012**, *2*, 1765−1768.
(16) Mahmoudi, M.; Shokrgozar, M. A. *Chem. Commun.* **2012**, *48*, 3957−3959.
(17) Yang, J. P.; Zhang, F.; Chen, Y. R.; Qian, S.; Hu, P.; Li, W.; Deng, Y. H.; Fang, Y.; Han, L.; Luqman, M.; Zhao, D. Y. *Chem. Commun.* **2011**, *47*, 11618−11620.
(18) Zhang, F.; Braun, G. B.; Shi, Y. F.; Zhang, Y. C.; Sun, X. H.; Reich, N. O.; Zhao, D. Y.; Stucky, G. *J. Am. Chem. Soc.* **2010**, *132*, 2850−2851.
(19) Deng, W.; Jin, D. Y.; Drozdowicz-Tomsia, K.; Yuan, J. L.; Wu, J.; Goldys, E. M. *Adv. Mater.* **2011**, *23*, 4649−4654.
(20) Wu, Z. Z.; Liang, J. L.; Ji, X. H.; Yang, W. S. *Colloids Surf., A* **2011**, *392*, 220−224.
(21) Guzatov, D. V.; Vaschenko, S. V.; Stankevich, V. V.; Lunevich, A. Y.; Glukhov, Y. F.; Gaponenko, S. V. *J. Phys. Chem. C* **2012**, *116*, 10723−10733.
(22) Bardhan, R.; Grady, N. K.; Halas, N. J. *Small* **2008**, *4*, 1716−1722.
(23) Evanoff, D. D.; White, R. L.; Chumanov, G. *J. Phys. Chem. B* **2004**, *108*, 1522−1524.
(24) Wang, Y. Q.; Chen, L. X.; Liu, P. *Chem.—Eur. J.* **2012**, *18*, 5935−5943.
(25) Bharadwaj, P.; Novotny, L. *Opt Express* **2007**, *15*, 14266−14274.
(26) Miao, X. Y.; Brener, I.; Luk, T. S. *J. Opt. Soc. Am. B* **2010**, *27*, 1561−1570.
(27) Marechal, X.; Mordon, S.; Devoisselle, J. M.; Begu, S.; Guery, B.; Neviere, R.; Buys, B.; Dhelin, G.; Lesage, J. C.; Mathieu, D.; Chopin, C. *Photochem. Photobiol.* **1999**, *70*, 813−819.